Modeling the Co-precipitation of Silica and Calcium Oxalate in Sugar Solutions

Christopher P. East[1], Christopher M. Fellows[2] and William O.S. Doherty[1]

[1]*Centre for Tropical Crops and Biocommodities, Queensland University of Technology, Brisbane,*

[2]*School of Science and Technology, The University of New England Armidale NSW*

Abstract

Solution chemistry plays a significant role in the rate and type of foulant formed on heated industrial surfaces. This paper describes the effect of sucrose, silica (SiO_2), Ca^{2+} and Mg^{2+} ions, and trans-aconitic acid on the kinetics and solubility of SiO_2 and calcium oxalate monohydrate (COM) in mixed salt solutions containing sucrose and refines models previously proposed. The developed SiO_2 models show that sucrose and SiO_2 concentrations are the main parameters that determine apparent order (n) and apparent rate of reaction (k) and SiO_2 solubility over a 24 h period. The calcium oxalate solubility model shows that while increasing [Mg^{2+}] increases COM solubility, the reverse is so with increasing sucrose concentrations. The role of solution species on COM crystal habit is discussed and the appearance of the uncommon (001) face is explained.

Keywords: Calcium oxalate; Silica; Composite fouling; Kinetics; Crystallization; Modeling

Introduction

The processing of natural aqueous feedstocks (e.g., sugar cane juice, beer and ground water) inevitably leads to the fouling of plant equipment and loss of heat transfer capacity in heat exchangers. The role of silica (SiO_2) fouling in the chemical industry is well documented and its deposition on surfaces poses some significant challenges in the efficient operation of plant equipment (Muller-Steinhagen, 2000; Neofotistou and Demadis, 2004; Ning, 2003; Sheikholeslami and Tan, 1999). Co-precipitation with other salts increases the complexity of the problem as these salts, e.g., calcium salts, are able to strengthen (through intergrowth) the SiO_2 deposits or cover the deposits (layering). This makes chemical cleaning more expensive and time consuming as more than one type of cleaning agent is required (East et al., 2011a, b).

Recently East *et al.* (2013) studied the effect of solution composition on the kinetics and thermodynamics of the co-precipitation of calcium oxalate (monohydrate, COM) and SiO_2 in sugar solutions, commonly found in the evaporators of Australian sugar factories. Table 1 shows the conditions for the laboratory tests (at two SiO_2 supersaturation ratios (SS)) used in that study. Equations 1-4 show the preliminary models that were generated for SiO_2 apparent order (n) and apparent rate (k) of reaction and solubility after 24 h ($[SiO_2]_{24}$) as well as the solubility of Ca^{2+} ($[Ca^{2+}]_{eq}$). Equation 5 was fitted to the SiO_2 concentration time series to generate values for n and k.

Table 1 Test scheme for the generation of the preliminary model

Component	Concentrations
Sucrose ([Suc])	25 and 40 wt/v%
Silica ($[SiO_2]$)	[Suc] = 25 wt/v%: 320 and 400 $mg \cdot L^{-1}$ (SS = 1.8 and 2.3) [Suc] = 40 wt/v%: 250 and 320 $mg \cdot L^{-1}$ (SS = 1.8 and 2.3)
Calcium ($[Ca^{2+}]$)	41 and 200 $mg \cdot L^{-1}$
Magnesium ($[Mg^{2+}]$)	0 and 84 $mg \cdot L^{-1}$
trans-Aconitic acid ([*t*AC])	0 and 1300 $mg \cdot L^{-1}$
Oxalate ($[C_2O_4^{2-}]$)	90 $mg \cdot L^{-1}$

$$n = -13.2 + 65.7 \times 10^{-3}[\text{Suc}] + 56.4 \times 10^{-3}[SiO_2] + 36.7 \times 10^{-3}[Mg^{2+}] - 53.0 \times 10^{-6}[SiO_2]^2 - 99.9 \times 10^{-6}[SiO_2][Mg^{2+}] \quad \text{(Eq 1)}$$

$$k = -6.01 \times 10^{-3} - 5.28 \times 10^{-6}[Ca^{2+}] + 41.1 \times 10^{-6}[\text{Suc}] + 17.2 \times 10^{-6}[SiO_2] - 0.166 \times 10^{-6}[t\text{AC}] + 0.148 \times 10^{-6}[Ca^{2+}][\text{Suc}] + 1.87 \times 10^{-9}[Ca^{2+}][t\text{AC}] \quad \text{(Eq 2)}$$

$$[SiO_2]_{24} = 1090 - 72.3 \times 10^{-3}[Ca^{2+}] - 4.08[\text{Suc}] - 3.93[SiO_2] - 1.19[Mg^{2+}] + 4.70 \times 10^{-3}[SiO_2]^2 + 3.22 \times 10^{-3}[SiO_2][Mg^{2+}] \quad \text{(Eq 3)}$$

$$[Ca^{2+}]_{eq} = -28.3 + 0.949[Ca^{2+}] - 0.101[\text{Suc}] + 0.116[Mg^{2+}] + 5.92 \times 10^{-3}[t\text{AC}] - 3.36 \times 10^{-3}[Ca^{2+}][\text{Suc}] - 0.668 \times 10^{-3}[Ca^{2+}][Mg^{2+}] - 48.3 \times 10^{-6}[Ca^{2+}][t\text{AC}] \quad \text{(Eq 4)}$$

The equations showed that *t*AC had little effect on the system given how much it is expected to vary in the process ($[Ca^{2+}]_{eq} \pm 1.5$ mg.L^{-1}, $k \pm 7\%$) (East et al., 2013). Also, values for $[Mg^{2+}]$ used by East et al. (2013) only represented the minimum $[Mg^{2+}]$ found in sugar cane juices (East et al., 2012; Thai and Doherty, 2011).

The present study is an advancement of the present knowledge on the co-precipitation of silica and calcium oxalate by: (a) developing a three-point non-linear and robust model, instead of the two-point linear model developed by East et al. (2013), to effectively describe and predict the co-precipitation of silica and calcium oxalate in synthetic sugar juice solutions; (b) using realistic $[Mg^{2+}]$ and [*t*AC] and including intermediate [Suc], $[SiO_2]$ and $[Ca^{2+}]$ values to mimic different types of sugar cane juice, (c) verifying the models with experimental data, and (d) studying COM crystal habits and growth in more complex synthetic juice solutions.

Experimental

Materials

Concentrated stock solutions of $CaCl_2 \cdot 2H_2O$ (Chem Supply, Gillman, Australia), $Na_2C_2O_4$ (Sigma-Aldrich, Sydney, Australia), Na_2SiO_3 (Sigma-Aldrich, Sydney, Australia), $MgCl_2 \cdot 6H_2O$ (Merck, Kilsyth, Australia), HCl and NaOH were prepared from analytical reagent grade chemicals (Merck, Kilsyth, Australia) dissolved in CO_2-free distilled water. *trans*-Aconitic acid, *t*AC (Sigma-Aldrich,

Sydney, Australia) and sucrose (Merck, Kilsyth, Australia) used in this study was analytical grade and the sucrose did not contain any measurable amounts of oxalic acid or other organic acids.

Test Scheme

A face-centred central composite design (CCD) was used to investigate the effect of change in concentration of four solution components (Table 2) on the formation of calcium oxalate and SiO_2. The lower and upper concentrations selected for sucrose are similar to the concentrations of sucrose entering the 3rd and 4th effects of an Australian sugar factory with a quintuple evaporator set, respectively. The concentration of silica ([SiO_2]), oxalate ([$C_2O_4^{2-}$]) and *trans*-aconitic acid ([*t*AC]) cover the general concentration range found in juices entering the 3rd and 4th effects of the same evaporator set. SiO_2 SS was used as a test parameter instead of concentration due to the significant reduction in solubility of SiO_2 caused by the high concentrations of sucrose (Yu et al., 2003). This is intended to keep the "driving force" for silicic acid polymerization constant over the test series so the effects of other components can be seen. The calcium concentration limits were selected to give a molar ratio of 1:1 and 5:1 [Ca^{2+}] to [$C_2O_4^{2-}$]. The Ca^{2+} and Mg^{2+} ion concentrations selected cover the levels found in syrups in Australian sugar factories (East et al., 2012; Thai and Doherty, 2011). The design consisted of a 2^p factorial augmented by 2p axial points and a centre point, where p is the number of varied solution constituents (p = 4). For this study, a total of 27 experiments were conducted with 16 factorial points, 8 axial points and 1 centre point replicated 3 times for experimental error calculation.

SiO_2 *n*, *k* and solubility after 24 h were determined for each test along with the [Ca^{2+}] at equilibrium and were used as the responses for the CCD.

Table 2 Values for the independent variables of the central composite design†

Component (mg.L^{-1})	**-1**	**0**	**1**
[Suc]	25 wt/v%	32.5 wt/v%	40 wt/v%
Silica SS*	SS = 1.8	SS = 2.05	SS = 2.3
[SiO_2] in 25 wt/v% sucrose	320	360	400
[SiO_2] in 32.5 wt/v% sucrose	270	310	350
[SiO_2] in 40 wt/v% sucrose	250	290	320
[Ca^{2+}] mg.L^{-1}	41	125	200
[Mg^{2+}] mg.L^{-1}	0	126	252
[*t*AC] mg.L^{-1}	1300	1300	1300
[$C_2O_4^{2-}$] mg.L^{-1}	90	90	90

†Tests conducted at 60 ºC and pH = 6

*Values of SiO_2 in mg.L^{-1} were used for the modeling. SiO_2 solubility changes with [Suc] (Yu et al., 2003)

Methodology

Sucrose, Ca^{2+} and Mg^{2+} ions and *trans*-aconitic acid were mixed in CO_2-free water (~350 mL) at 60 °C and the pH was adjusted to 6.0 using a portable pH meter (Hach H160, Loveland, Co, USA) with an Ionode PBFC single junction Ag/AgCl pH probe with saturated KCl reference solution, which was calibrated before each test using Isolab pH 4.01 ± 0.02 at 25 ºC and 7.00 ± 0.02 at 25 ºC buffer solutions. Sodium oxalate (90 mg·L^{-1} $C_2O_4^{2-}$ in the final solution) and SiO_2 solutions (at 60 °C) were placed in separate beakers, their pHs were adjusted to 6.0 and added at the same time to the sucrose solution containing the other compounds. The solution was quickly made up to 500 mL and transferred to capped 15 mL plastic tubes. The tubes were then placed in a water bath at 60 °C. Samples were taken after 20, 40 and 60 minutes, followed by one sample every hour, and analyzed. The use of a water bath does not represent the fouling environment in sugar factory evaporators, which have a temperature gradient at the tube walls. However, Yu (2003) found no significant difference using a water bather and a single heated tube on the co-precipitation of silica and calcium oxalate. Tests were stopped after 24 h because of the hydrolysis of

sucrose. It was found in a separate experiment that 40 wt/v% sucrose solution degraded by 2 %, 16% and 34% after 10 h, 24 h and 120 h respectively in solutions containing Ca, $C_2O_4^{2-}$, SiO_2 and *t*AC (East et al., 2013).

Samples were analyzed for reactive [SiO_2], [Ca^{2+}] and [$C_2O_4^{2-}$] as described by Yu *et al*. (2002, 2003). Reactive silica was analyzed with a Cintra 40 double-beam UV-Visible spectrometer (GBC Scientific Equipment Pty. Ltd., Braside, VIC, Australia) using the silica-molybdate complex colorimetric method (APHA, 1996). The samples were filtered through 0.2 μm membrane filters and [Ca^{2+}] and [$C_2O_4^{2-}$] were determined from the filtrate. Oxalate ion concentration was determined by UV-Vis using a colorimetric method (Burriel-Martí et al., 1953). However, it could not be accurately determined because of significant interferences when *t*AC and Mg^{2+} ions were present, and so the data obtained was not used in this work. Ca^{2+} ion concentrations were determined using inductively coupled plasma – optical emission spectroscopy (ICP-OES Vista MPX, Varian Inc., Mulgrave, VIC, Australia).

Analysis of Calcium Oxalate Crystals

After 24 h, samples were centrifuged and washed with Millipore water, then with ethanol (96%, Merck, Kilsyth, Australia) and oven dried at 40 ºC. X-ray powder diffraction (XRD) was conducted using PANalytical X'Pert MPD XRD equipment emitting Cu K_α (1.5418 Å) radiation. The x-ray patterns were indexed on the basis of parameters obtained from the International Centre for Diffraction Data powder XRD card index.

Samples for energy dispersive spectroscopy (EDX) analysis were dispersed on an aluminum stub in ethanol and air dried. They were examined uncoated, under low vacuum, in an FEI Quanta 3D scanning electron microscope (SEM) with a 15 kV beam energy. EDX spectra were collected with an EDAX 30 mm^2 SiLi detector, and EDAX Genesis software (v5.11).

Statistical Analysis

The rate equation generally used to describe the kinetics of polymerization reaction is given by:

$$\frac{dC_t}{dt} = -k\left(\frac{C_t - C_e}{C_e}\right)^n \quad \text{(Eq 5)}$$

where k is the apparent rate constant ($mol \cdot L^{-1} \cdot h^{-1}$), n is the apparent order of reaction, C_t is the concentration at time t and C_e is the equilibrium concentration determined experimentally for each [Suc]. n and k for silicic acid polymerization were determined using a simulated annealing algorithm using the ODE 45 function in MatLab (The MathWorks, v 7.10.0.499) to find the optimal values (Corana et al., 1987). It was not possible to accurately determine the apparent order and rate of reaction for calcium oxalate because the rate of reaction was very fast.

Response surfaces were then fitted to n, k and solubility values (using MiniTab v16.0) to generate equations that describe the relationship the juice constituents have on n, k and on the solubilities of SiO_2 and calcium oxalate. Analysis of variance (ANOVA) was used for model adequacy and significance of the experimental data. The quality of the fitted model was expressed by the regression coefficient, R^2, and its statistical significance was checked by the Fisher's F-test. Model terms were determined based on the significance of each term at a confidence level of 95%. This was evaluated by examining its respective P value (probability), where the smaller the P value, the more significant its corresponding coefficient and the interaction effect with the response. The models were developed using an iterative method where insignificant terms ($P > 0.05$) were dropped and the model was refitted to give a better fit and more accurate coefficients. The ANOVA results for the quadratic model results for n and k for silicic acid polymerization, solubility of SiO_2 after 24 hours ($[SiO_2]_{24}$) and apparent solubility of calcium oxalate based on calcium ion equilibrium concentration ($[Ca^{2+}]_{eq}$) can be found in Supplementary data; Tables S1 – S4.

Results

Silicic Acid Polymerization Kinetics

Table 3 shows the n and k values for silicic acid polymerization determined by an annealing fitting method. The results show the effect of $[SiO_2]$ SS and [Suc] on the values of n and k. Variations due to changes in the $[Ca^{2+}]$ and $[Mg^{2+}]$ have not been included because the model shows that neither variable significantly changes the n

and *k* values. Equations 6 and 7 are the models generated for apparent *n* and apparent *k* for silicic acid polymerization, showing the relationship between them and the initial solution concentrations of the different components. As these models were generated with a wider range of data set, it was not necessary to over fit the data to improve their accuracy.

Table 3 Silicic acid polymerization kinetics data in calcium oxalate and silica systems as described by Table 2*

[Suc]	SiO_2 SS = 1.8		SiO_2 SS = 2.05		SiO_2 SS = 2.3	
wt/v%	*n*	*k* ($\times 10^{-3}$)	*n*	*k* ($\times 10^{-3}$)	*n*	*k* ($\times 10^{-3}$)
25	1.6-2.2	0.2-0.3	2.3†	0.5†	2.6-3.0	0.9-1.2
32.5	0.5†	0.1†	1.0-2.4	0.2	3.1†	0.2†
40	0	0-0.1	1.4†	0.2†	2.6-2.8	0.5-0.9

*Error to determine *n* and *k* is ± 10%

†Single values

$$n = 6.25 - 0.359[\text{Suc}] - 0.0179[SiO_2] + 1.27 \times 10^{-3}[\text{Suc}][SiO_2] \quad \text{(Eq 6)}$$

$R^2 = 0.768$

$$k = 0.0199 - 0.528 \times 10^{-3}[\text{Suc}] - 80.7 \times 10^{-6}[SiO_2] + 4.14 \times 10^{-6}[\text{Suc}]^2 + 94.1 \times 10^{-9}[SiO_2]^2 + 0.889 \times 10^{-6}[\text{Suc}][SiO_2] \quad \text{(Eq 7)}$$

$R^2 = 0.881$

In comparison to the models of Equations 1 and 2, these models have fewer terms making them easier to use. The chemical interactions between SiO_2-Mg^{2+}-$C_2O_4^{2-}$, SiO_2-Ca^{2+} and SiO_2-*t*AC that were evident in the previous models may still a play role, though of an insignificant nature in the prediction of the *n* and *k* values within the concentration range studied. The data shows that increasing [SiO_2] increases both *n* and *k*, which is due to solubility effects and that increasing the [Suc] at a fixed SiO_2 SS decreases both *n* and *k*. Yu *et al.* (2003) found that increasing the [Suc] increased *k* and decreased *n*. Whilst this data is in agreement with Yu *et al.* with regards to *n* it differs with respect to *k*. The simplest explanation for this difference is the difference in experimental procedure where Yu *et al.* ran tests up to 450 h while

the tests in this study were terminated after 24 h in order to prevent sucrose degradation and change the chemistry of the systems (East et al., 2013). Increasing the amount of [Suc] increases the viscosity of the solution and reduces diffusion of particles through the solution. As such, a drop in n implies that the polymerization process changes from surface-controlled and poly-nuclear mechanisms ($n = 2$ and $n \geq 3$ respectively) to a mechanism controlled by bulk diffusion ($n = 1$) (Nancollas et al., 1991). A drop in k is the result of the increased viscosity in the solution.

Figures 1 and 2 show the calculated (i.e., model) vs measured n and k values for silicic acid polymerization respectively. Both models show a linear relationship with the model for n having a gradient of 1 and an intercept of 0. The model fits values of n above 2 well and reasonably well for values between 1.5 and 2. The model for n does not well model values of $n < 1$, which is due to the slowness of the reaction rates. Increasing the reaction time to allow for the processes to come to completion was unacceptable due to the degradation of sucrose (16% and 34% loss after 24 and 120 h respectively). The linear relationship for k is ~1 and the intercept is near zero, which shows that the model accounts for nearly all the variation in the data.

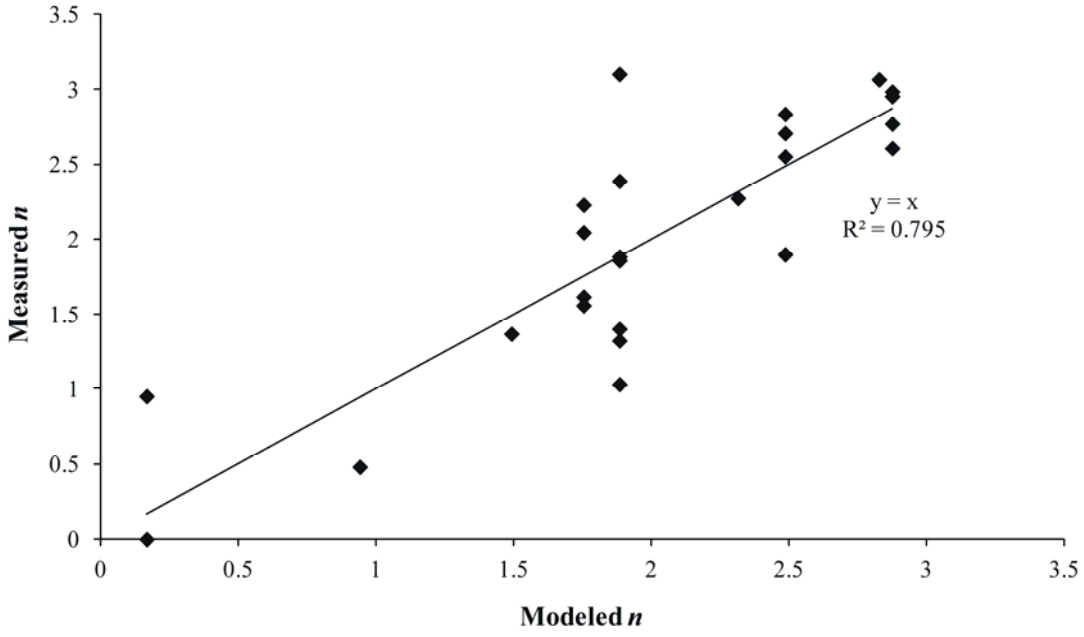

Figure 1 Modeled vs measured *n* for silicic acid polymerization

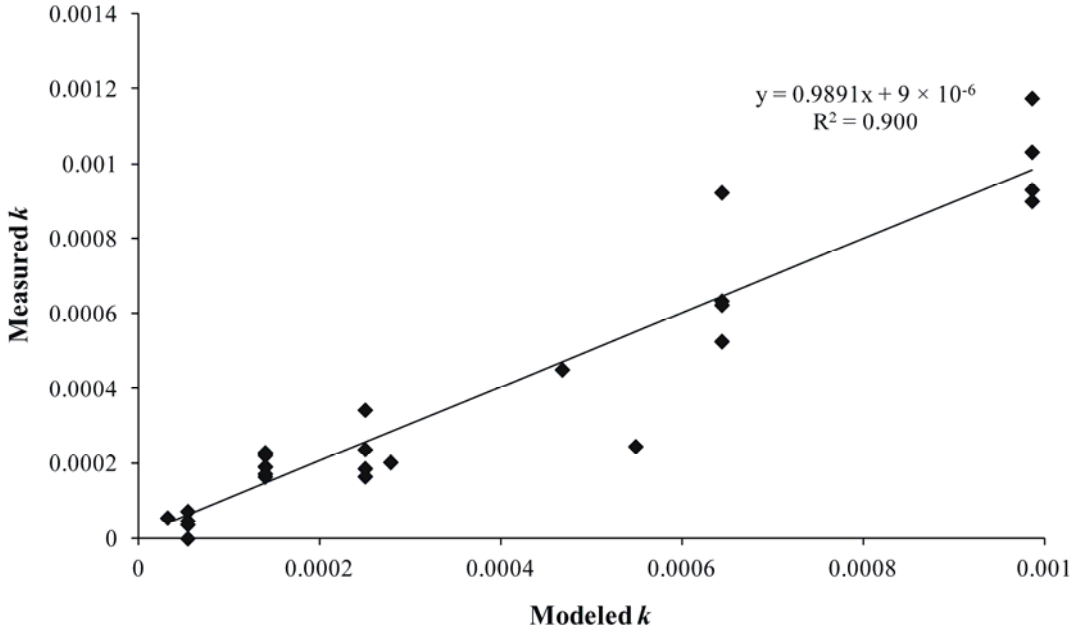

Figure 2 Modeled vs measured *k* for silicic acid polymerization

Silica Solubility

Equation 8 shows the relationship generated by the response surface methodology between the solubility of SiO_2 after 24 h of polymerization ($[SiO_2]_{24}$) and the initial solution concentrations of the different components.

$$[SiO_2]_{24} = 906 - 4.05[Suc] - 3.09[SiO_2] + 3.78 \times 10^{-3}[SiO_2]^2 \quad \text{(Eq 8)}$$

$R^2 = 0.772$

Figure 3 shows the modeled vs measured solubility data for silica at 24 h. The data sets show good agreement, which indicates that the model is a good fit for estimating SiO_2 solubility. Increasing both $[SiO_2]$ and [Suc] reduce the value of $[SiO_2]_{24}$. It is important to note however, that this is not the equilibrium solubility and that increasing the initial $[SiO_2]$ does not decrease the solubility but rather brings the reaction to equilibrium faster. Increasing the initial concentration of sucrose has a large effect on silica solubility reducing it from 175 $mg.L^{-1}$ at 25 wt/v% to 140 $mg.L^{-1}$ at 40 wt/v% (Yu, 2003).

There are a number of differences between this model and the previous one (Equation 3). Firstly, the previous model has many variables. Adding the centre term to this model has shown that perhaps, though unlikely, the weakly significant

(P = 0.020) [Ca^{2+}] term in the previous model may not be significant. The extended [Mg^{2+}] range used in the present set of experiments appears to show that [Mg^{2+}] is not a significant factor in determining the solubility of silica up to 24 h.

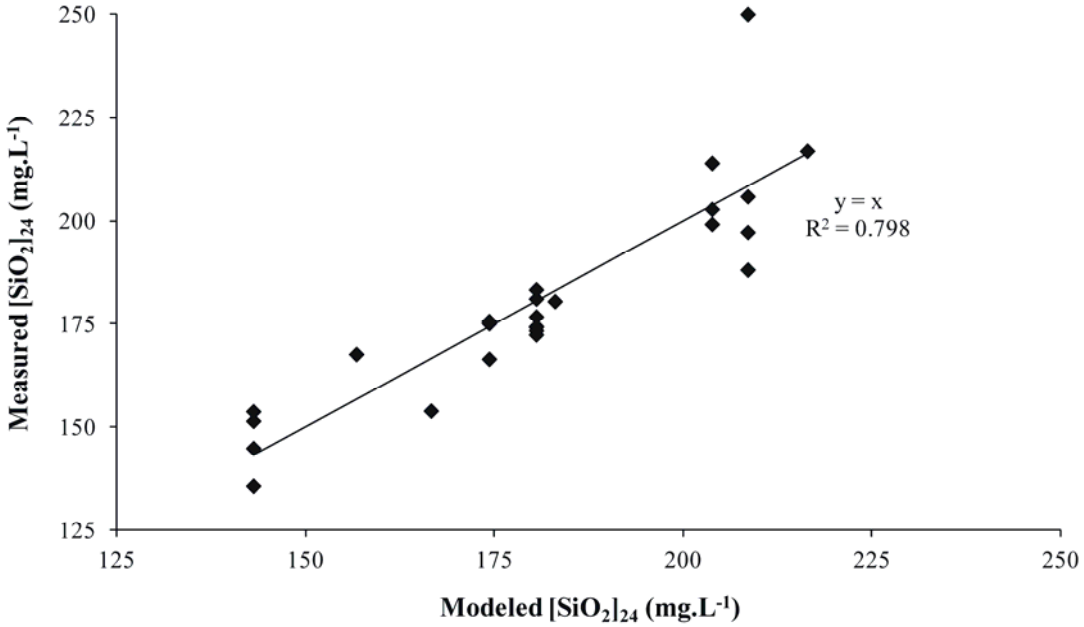

Figure 3 Modeled vs measured $[SiO_2]_{24}$

Calcium Oxalate

Calcium oxalate crystallized very quickly and so it is not possible to obtain n and k values using the methods described in this work. Equation 9 shows the relationship generated by the response surface methodology between the apparent equilibrium solubility of calcium oxalate on the basis of the concentration of calcium ions in solution ($[Ca^{2+}]_{eq}$), with a constant initial concentration of oxalate (90 mg·L^{-1}), and the initial solution concentrations of the different components.

$$[Ca^{2+}]_{eq} = -16.1 + 0.0165[Suc] + 0.671[Ca^{2+}] + 0.133[Mg^{2+}] + 0.914 \times 10^{-3}[Ca^{2+}]^2 - 3.82 \times 10^{-3}[Suc][Ca^{2+}] - 0.522 \times 10^{-3}[Ca^{2+}][Mg^{2+}] \quad \text{(Eq 9)}$$

$R^2 = 0.995$

Figure 4 shows the modeled vs the measured data for Ca^{2+} ion equilibrium concentration using Equation 9. The two data sets are in good agreement and show

values similar to those in those reported in previous study (East et al., 2013). Increasing the [Mg^{2+}] increases the solubility of calcium oxalate mainly because of complex formation between Mg^{2+} and $C_2O_4^{2-}$ ions, resulting in more Ca^{2+} ions remaining in solution as result of chelation with *t*AC (Desmars and Tawashi, 1973; Doherty, 2006; East et al., 2013; Graddon, 1956; Oka et al., 1987). The reduction of $C_2O_4^{2-}$ ions through complex formation with Mg^{2+} is reduced at higher initial [Ca^{2+}] probably because of preferential binding of the latter to $C_2O_4^{2-}$ ions. Increasing [Suc] decreases the calcium oxalate solubility (more so at higher [Suc]), which is in good agreement with Yu *et al*. (2003) and previous work by the authors (East et al., 2013). There are no major differences between the Ca^{2+} solubility model and the model developed in previous work of the authors (East et al., 2013).

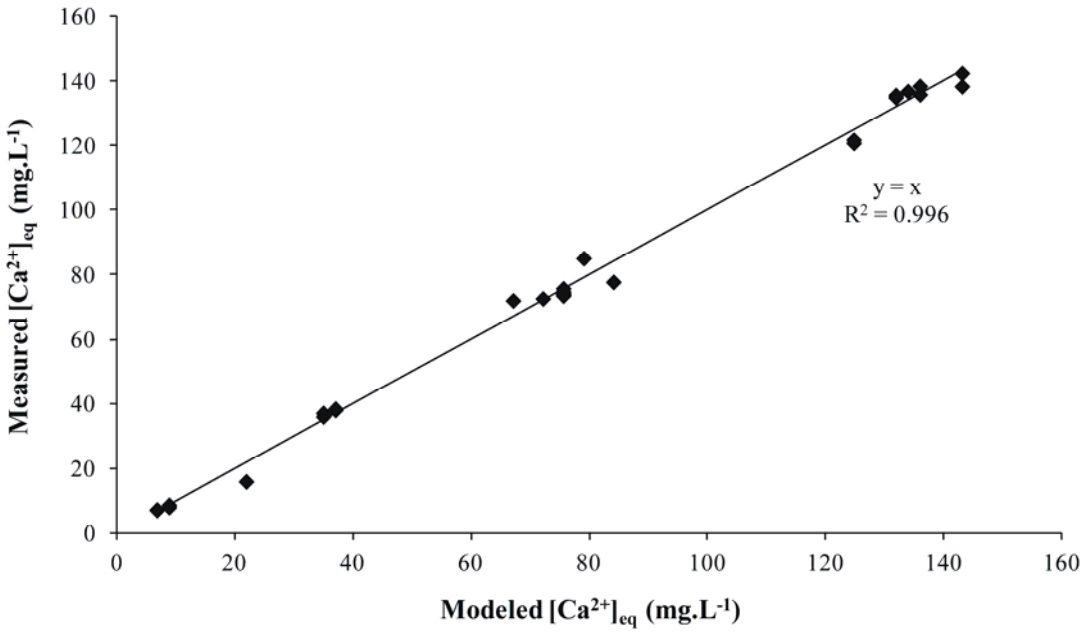

Figure 4 Modeled vs measured $[Ca^{2+}]_{eq}$

Verification of Models

As shown in Table 4, the four models (described previously) were tested with starting solution concentrations designed to give the maximum and minimum value for each model (*i.e.*, maximum and minimum $[Ca^{2+}]_{eq}$, $[SiO_2]_{24}$, *n*, and *k*) and two other values, giving four tests in total.

Table 5 shows the predicted and measured values for each test and the percentage differences. In most cases, there are good agreement between the values

obtained with the models and the measured values despite working in very complex systems. There are significant differences in the predicted and measured values of $[Ca^{2+}]_{eq}$ and k for test 2. For this system the $[Mg^{2+}]$ is ~3 times that of $[Ca^{2+}]$ and so with such abundance of Mg^{2+} ions there may well be interactions not only between Mg^{2+} and $C_2O_4^{2-}$ ions and between Mg^{2+} ions and SiO_2, but other interactions between the species in solution that the developed models cannot account for.

The models do not well predict small values of n (Table 5 row 10 and 11) and k (Table row 14 and 15) well. The most likely explanation lies with the data and the "speed" of reaction at low supersaturation. For tests with low starting SiO_2 SS a curve is fitted to what could be approximated to a straight line, causing error in the fitting. It should also be noted that solutions with low SiO_2 SS have relatively long induction times (h) which may effect silicic acid polymerization and hence the validity of the models.

Table 4 Model test parameters*

Test	[Suc] (wt/v%)	$[SiO_2]$ ($mg.L^{-1}$)	$[Ca^{2+}]$ ($mg.L^{-1}$)	$[Mg^{2+}]$ ($mg.L^{-1}$)	Min	Max
1	40	250	40	0	$[Ca^{2+}]_{eq}$, n	$[SiO_2]_{24}$
2	32.5	270	40	126	k	
3	25	400	200	252		$[Ca^{2+}]_{eq}$, n, k
4	40	320	125	84	$[SiO_2]_{24}$	

*$[t\text{AC}] = 1300\ mg.L^{-1}$; $[C_2O_4^{2-}] = 90\ mg.L^{-1}$; pH 6.0; 60 ºC

Table 5 Model verification results

	Test	Predicted	Measured	Difference (%)
$[Ca^{2+}]_{eq}$	1	6.8	6.0	-11.5
($mg.L^{-1}$)	2	21.9	10.0	-54.3
	3	143.1	152.9	6.85
	4	69.3	77.6	12.0
$[SiO_2]_{24}$	1	209	195	-6.29
($mg.L^{-1}$)	2	216	212	-2.18
	3	174	184	5.53
	4	143	160	11.7
n	1	0.167	0.657	294
	2	0.941	0.960	1.99
	3	2.87	2.56	-10.9
	4	2.49	2.65	6.66
k ($\times 10^{-5}$)	1	5.40	6.43	19.0
($mol.L^{-1}.h^{-1}$)	2	3.16	6.81	115
	3	98.6	100	1.46
	4	64.3	52.8	-17.9

Calcium Oxalate Precipitates

Scanning electron micrographs (Figure 5) and XRD patterns (Figure 6) of crystals were obtained from the present study and those from the previous study (East et al., 2013) under the test conditions in Table 6. Typical synthetic COM crystals form monoclinic boat or plate-like crystals with (100), (010) and $(1\bar{2}1)$ faces (Figure 7(B)) (Millan, 2001). In the present and previous studies, solutions containing only sucrose and SiO_2 forms the typical boat shaped crystals (Figure 5(a)) with some crystal twining (Figure 8), probably due to the rate of crystallization and temperature variation (Millan, 2001). When 1300 $mg.L^{-1}$ *t*AC is added to the solution containing sucrose and SiO_2, COM crystal twining is increased (Figure 5(b)). This indicates a reduction in available nuclei able to grow during the initial stages of crystallization (Tunik et al., 1996) and chelation between Ca^{2+} ions and *t*AC. Recently East et al.

(2010) showed that *trans*-aconitic acid has the ability to promote COD formation in sucrose solutions, with higher concentrations of sucrose yielding more COD. This is probably due to *trans*-aconitic acid adsorbing to the COM crystal surfaces and blocking growth as COM crystals are more adsorbing than COD crystals (Tunik et al., 1998). It may also be due to the ability of carboxylic acids to form chelates with calcium restricting the amount of water of hydration surrounding Ca^{2+} ions (Doherty et al., 1994). This allows COD crystals to grow in preference of COM. However in the present studies no detectable COD crystals were found.

The addition of 84 $mg.L^{-1}$ Mg^{2+} ions to a solution containing sucrose and SiO_2 changes the COM crystal habit to an equilibrium penetration twin (Figure 5(c) and Figure 8) with the emergence of the (021) crystal face. Increasing the $[Mg^{2+}]$ in solution to 126 $mg.L^{-1}$ (or higher) the crystal habit changes to a rectangular prism, in the presence or absence of *t*AC (Figure 5(d)). The rectangular prisms have the (100), (010) and the (001) faces and are a modified version of Figure 7(A). Tunik *et al.* (1998) showed that the (010) faces are characterized by $C_2O_4^{2-}$ ions lying perpendicular to the face alternating with those parallel to the face and the (100) faces are characterized by $C_2O_4^{2-}$ ions emerging oblique to the faces with a dense pattern of complexed calcium ions exposed on the surface. The (001) face was not examined by Tunik *et al*. (1998) as it is rare to find it in synthetic crystals (Millan, 2001). However, it appears that the $C_2O_4^{2-}$ ions emerge perpendicular (length wise) to or lie on the surface (Tunik et al., 1998). It is quite possible that Mg^{2+} ions are complexing with $C_2O_4^{2-}$ ions to the crystal surface instead of Ca^{2+} ions and hence blocking COM growth on those faces. In the presence of *t*AC crystal inhibition on these faces is increased because tAC is complexing to both Mg^{2+} and Ca^{2+} ions.

It also important to note that the crystals were grown over a 24 h period, allowing the stable $(1\bar{2}1)$ and (021) crystal faces to develop (Millan, 2001). However, due to the attached complexes on the (100) and (010) faces restricting growth on these faces, the $(1\bar{2}1)$ and the (021) faces slowly grow and eventually disappear with the emergence of the (001) face. The crystals in Figure 5(e) are from a verification test showing the repeatability of the formation of the (001) face.

376

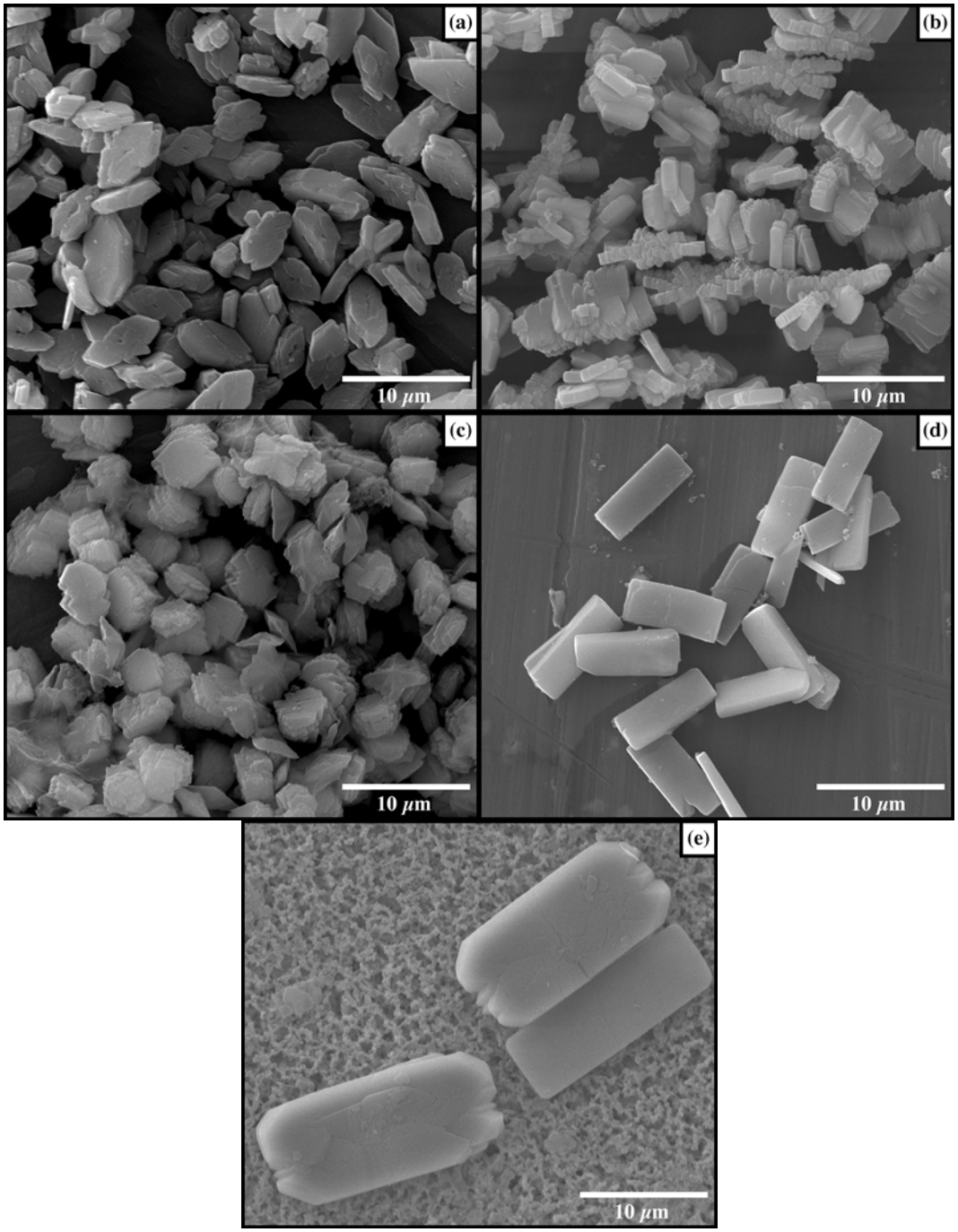

377

378

379 **Figure 5 Different forms of COM crystal habit**

380

381

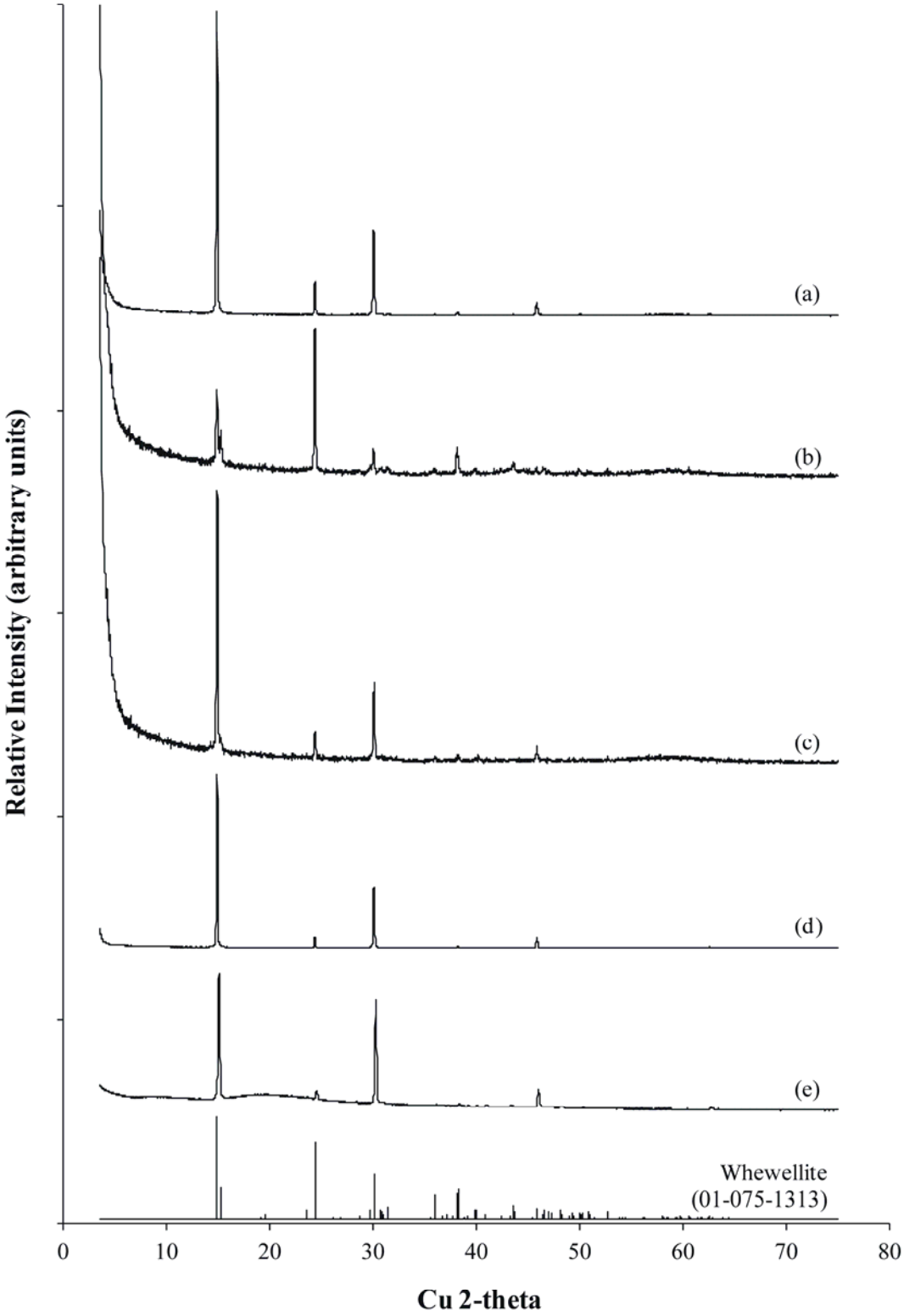

382

383 **Figure 6 Typical XRD patterns of COM crystals**

384

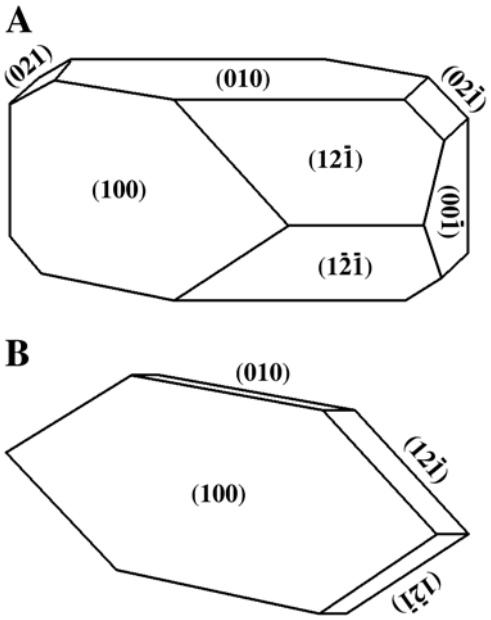

Figure 7 COM crystals showing (A) possible equilibrium shape (B) typical synthetic COM crystals (Millan, 2001)

Table 6 Test conditions for the crystals in Figures 5 and 6

Test	Suc (w/v%)	SiO_2 ($mg.L^{-1}$)	Ca^{2+} ($mg.L^{-1}$)	*t*AC ($mg.L^{-1}$)	Mg^{2+} ($mg.L^{-1}$)
a	25	400	41	0	0
b	25	320	200	1300	0
c	25	400	200	0	84
d	32.5	310	125	1300	126
e	32.5	270	40	1300	126

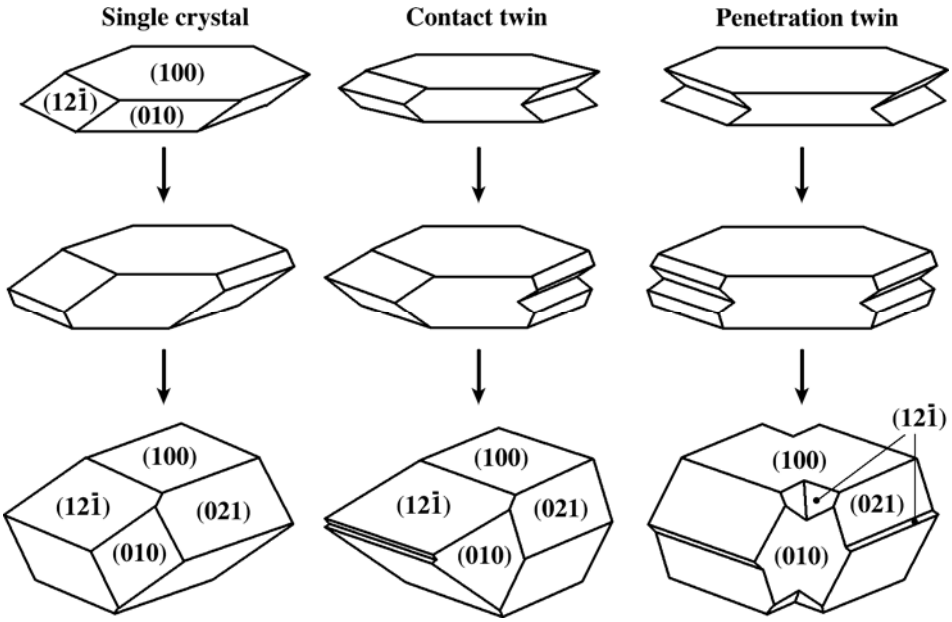

Figure 8 COM single crystal and twins growth (Millan, 2001)

Conclusions

This work has attempted to develop models for the kinetics and solubility of SiO_2 and COM co-precipitation in synthetic sugar solutions at a pH 6 at 60 ºC . The models show that [Suc] and [SiO_2] are the main parameters that determine *n*, *k* and SiO_2 solubility over a 24 h period. The factors that determine COM equilibrium solubility are [Suc], [Mg^{2+}] and initial [Ca^{2+}]. *trans*-Aconitic acid and Mg^{2+} ions have been shown to effect the habit of COM crystals. *trans*-Aconitic acid increases crystal twining and secondary nucleation, while the addition of small amounts of Mg^{2+} ions encourages the formation of double penetration twins. When the [Mg^{2+}] is further increased the crystal habit changes to that of a rectangular prism with (100), (010) and the synthetically uncommon (001) faces, along with some (021) and ($1\bar{2}1$) faces in crystals that were not fully grown.

Acknowledgments

This work was supported by the Australian Research Linkage grant, Mulgrave Central Mill and Sugar Research Limited. Many thanks go the Mr Tony Raftery of the X-ray and Microscopy Centre at Queensland University of Technology, Brisbane, Australia for his assistance in XRD analyses. Thanks also go to Dr James McGree, Mathematical Sciences, Queensland University of Technology, Brisbane, Australia for his assistance in processing the kinetic data.

References

APHA, (1996). Standard methods for the examination of water and wastewater. APHA-AWWA-WEF, Washinton, D. C.

Burriel-Martí, F., Ramírez-Munõz, J., Fernańdez, E., (1953). Determination of oxalate ion and calcium ion by indirect colorimetry. *Analytical Chemistry* 25, 583-585.

Corana, A., Marchesi, M., Martini, C., Ridella, S., (1987). Minimizing multimodal functions of continuous variables with the 'simulated annealing' algorithm. *Transactions on Mathematical Software* 13(3), 262-280.

Desmars, J.F., Tawashi, R., (1973). Dissolution and growth of calcium oxalate monohydrate I. Effect of magnesium and pH. *Biochimica et Biophysica Acta (BBA) - General Subjects* 313(2), 256-267.

Doherty, W.O.S., (2006). Effect of Calcium and Magnesium Ions on Calcium Oxalate Formation in Sugar Solutions. *Industrial and Engineering Chemistry Research* 45(2), 642-647.

Doherty, W.O.S., Crees, O.L., Senogles, E., (1994). The preparation of calcium oxalate dihydrate crystals. *Crystal Research and Technology* 29(4), 517-524.

East, C.P., Doherty, W.O.S., Fellows, C.M., Yu, H., (2010). Formation of thermodynamically unstable calcium oxalate dihydrate in sugar solutions. *Proceedings of the Australian Society of Sugar Cane Technologists* 32, 522-533.

East, C.P., Doherty, W.O.S., Fellows, C.M., Yu, H., (2011a). Characterization of sugar juice heat exchanger tube deposit. *Surface and Interface Analysis* 43(9), 1231-1239.

East, C.P., Doherty, W.O.S., Fellows, C.M., Yu, H., (2011b). Deposition of hydroxyapatite and calcium oxalate dihydrate on a heat exchanger tube. *Asia-Pacific Journal of Chemical Engineering* 6(6), 921-932.

East, C.P., Fellows, C.M., Doherty, W.O.S., (2012). Scale formation in sugarcane juice heat exchangers, in: Amjad, Z. (Ed.), *Mineral Scales in Biological and Industrial Systems*. CRC Press.

East, C.P., Fellows, C.M., Doherty, W.O.S., (2013). Aspects of kinetics and solubility of silica and calcium oxalate composites in sugar solutions. *Journal of Food Engineering* 117(3), 291-298.

Graddon, D.P., (1956). The absorption spectra of complex oxalates. *Journal of Inorganic and Nuclear Chemistry* 3, 308-322.

449 Millan, A., (2001). Crystal Growth Shape of Whewellite Polymorphs: Influence of
450 Structure Distortions on Crystal Shape. *Crystal Growth & Design* 1(3), 245-254.
451 Muller-Steinhagen, H., (2000). *Handbook heat exchanger fouling. Mitigation and*
452 *cleaning technologies.* Publico Publications, Essen, Germany.
453 Nancollas, G.H., Smesko, S.A., Campbell, A.A., Richardson, C.F., Johnsson, M.,
454 Iadiccico, R.A., Binette, J.P., Binette, M., (1991). Physical chemical studies of
455 calcium oxalate crystallization. *Am. J. Kidney Dis.* 17(4), 392-395.
456 Neofotistou, E., Demadis, K.D., (2004). Use of antiscalants for mitigation of silica
457 (SiO2) fouling and deposition: fundamentals and applications in desalination systems.
458 *Desalination* 167(0), 257-272.
459 Ning, R.Y., (2003). Discussion of silica speciation, fouling, control and maximum
460 reduction. *Desalination* 151(1), 67-73.
461 Oka, T., Yoshioka, T., Koide, T., Takaha, M., Sonoda, T., (1987). Role of Magnesium
462 in the Growth of Calcium Oxalate Monohydrate and Calcium Oxalate Dihydrate
463 Crystals. *Urologia Internationalis* 42(2), 89-93.
464 Sheikholeslami, R., Tan, S., (1999). Effects of water quality on silica fouling of
465 desalination plants. *Desalination* 126(1-3), 267-280.
466 Thai, C.C.D., Doherty, W.O.S., (2011). The composition of sugar cane juices derived
467 from burnt cane and whole green cane crop. *Proceedings of the Australian Society of*
468 *Sugar Cane Technologists* 33, 1-9.
469 Tunik, L., Addadi, L., Garti, N., Füredi-Milhofer, H., (1996). Morphological and
470 phase changes in calcium oxalate crystals grown in the presence of sodium diisooctyl
471 sulfosuccinate. *Journal of Crystal Growth* 167(3-4), 748-755.
472 Tunik, L., Füredi-Milhofer, H., Garti, N., (1998). Adsorption of Sodium Diisooctyl
473 Sulfosuccinate onto Calcium Oxalate Crystals. *Langmuir* 14(12), 3351-3355.
474 Yu, H., (2003). The mechanisms of composite fouling in Australian sugar mill
475 evaporators by calcium oxalate and amorphous silica, *School of Chemical*
476 *Engineering and Industrial Chemistry*. University of New South Wales, Sydney.
477 Yu, H., Sheikholeslami, R., Doherty, W.O.S., (2002). Mechanisms, thermodynamics
478 and kinetics of composite fouling of calcium oxalate and amorphous silica in sugar
479 mill evaporators—A preliminary study. *Chemical Engineering Science* 57(11), 1969-
480 1978.

Yu, H., Sheikholeslami, R., Doherty, W.O.S., (2003). Composite fouling of calcium oxalate and amorphous silica in sugar solutions. *Industrial and Engineering Chemistry Research* 42(4), 904-910.